Characterization of neutral boron-silicon clusters using infrared spectroscopy: The case of Si_6B

Nguyen Xuan Truong[a], Marko Haertelt[b], Bertram K.A. Jaeger[a], Sandy Gewinner[b], Wieland Schöllkopf[b], André Fielicke[a]*, and Otto Dopfer[a]*

a) Institut für Optik und Atomare Physik, Technische Universität Berlin, Hardenbergstraße 36, D-10623 Berlin, Germany

*) Email: fielicke@physik.tu-berlin.de, dopfer@physik.tu-berlin.de

b) Fritz-Haber-Institut der Max-Planck-Gesellschaft, Faradayweg 4-6, D-14195 Berlin, Germany

Abstract

Nano-size clusters are of great interest for understanding of fundamental properties and processes relevant for applied materials science such as heterogeneous catalysis. In this study, we present a newly developed dual-target dual-laser ablation source, suitable for the production of binary clusters and their spectroscopic characterization. With the current design, an almost arbitrary mixing ratio can be achieved by altering different parameters such as the laser fluences. Boron and silicon targets are chosen for cluster production, illustrating the possibility to control the outcome ranging from pure boron over mixed Si_nB_m to pure silicon clusters. As a test system, Si_6B clusters are characterized by means of infrared-ultraviolet two-color ionization (IR-UV2CI) spectroscopy, combined with quantum chemical simulations. The most stable structure of Si_6B (C_s, $^2A'$) predicted in our previous work is confirmed by the present experiment. Doping of Si_7 with a single B atom has a drastic impact on the geometric, vibrational, and electronic properties.

1. Introduction

Nano-size silicon-based structures have attracted a lot of interest in the current miniaturization trend toward nanophotonics and nanoelectronics (e.g., [1-5]). Particularly, the understanding of material properties changing with size, composition, and charge plays an important role. It has been shown that nanostructures such as metal and semiconductor nanocrystals, quantum dots, and nanowires can be well described within the context of related isolated (gas-phase) atomic clusters [2, 6, 7]. As pure gas-phase silicon clusters are chemically reactive, doping with other elements has been considered as a solution in finding stable Si-based building blocks [8, 9]. With the discovery of a superconducting transition at about 40 K in MgB_2 [10], there has been great interest in boron-doped materials as promising superconductors, including boron-doped diamond [11, 12], silicon [13], and silicon carbide [14-16]. In crystalline phases, doping of group IV elements with boron as the source of hole-doping has been shown to induce superconductivity [12, 13, 17]. For sufficient boron doping (~100 ppm), silicon becomes metallic [18] and superconducting at a boron concentration of several percent with a critical temperature of $T_c \approx 0.35$ K [13]. Ab initio calculations combined with Raman measurements strongly suggest that doping is substitutional [13]. Interestingly, similar effects have also been predicted for small B-doped silicon clusters [19]. Efforts have been made to increase T_c in B-doped silicon [16, 20, 21].

Studies on small B-doped silicon clusters are however rare, both in theory and experiment. For instance, heats of formation of gas-phase Si_nB (n=1-3) were measured by mass spectrometry [22]. Density functional theory (DFT) calculations for SiB_2, Si_2B, and Si_2B_2 found stable ring-like structures with strong π-bonding [23]. Anionic Si_nB^- clusters (n=1-6) formed by direct laser ablation from a mixed B/Si sample were studied by mass spectrometry and DFT calculations [24]. In that work, Si_6B^- was predicted to have C_{5v} symmetry ($^1A_1$), whereas its neutral counterpart was suggested to have C_s symmetric geometry ($^2A'$) [25]. Recently, Tam *et al.* studied thermochemical parameters and the growth mechanism of B-doped silicon clusters (Si_nB^q, n=1-10, q=0, ±1) using B3LYP, G4, and CCSD(T) approaches [19]. The ground state structures predicted for the neutrals suggest a growth mechanism, in which each Si_nB is formed by adding a Si atom to $Si_{n-1}B$ rather than adding B into Si_n. For Si_8B, exohedral and endohedral structures become close in energy. Interestingly, pure boron clusters with sizes of up to 20 atoms have quasi-planar structures, while SiB_7 was predicted to have a 3D structure [26], indicating the importance of a single dopant atom on the properties of pure clusters. Surprisingly, no spectroscopic data are available for B-doped silicon clusters in any charge state. Here, we combine infrared-ultraviolet two-color ionization (IR-UV2CI) spectroscopy [27] with quantum chemical simulations to determine the structure of Si_6B, a strategy recently applied to a variety of (doped) silicon clusters [25, 27-30].

Due to the high melting point of boron (> 2000°C), B-containing clusters are usually generated by laser ablation (see, e.g., [31, 32]). An exhaustive review of laser ablation sources has recently been provided by Duncan [33]. To produce mixed clusters, various approaches have been demonstrated, such as single targets of alloys [34], binary compounds [35-37], pressed mixed powders [38, 39], and dual-target (dual-laser) sources [40-44]. The dual-target dual-laser source designs allow for controlling the mixing ratios by changing the laser fluences, laser timing, and the rotation and/or translation speeds of the targets. Here, we describe a dual-target dual-laser ablation source developed for the production and spectroscopic measurement of binary clusters. We

demonstrate that with this cluster source an almost arbitrary mixing ratio between the different components can be achieved. As an example for the spectroscopic characterization of the clusters produced in this source, we apply the IR-UV2CI technique to neutral Si_6B to determine its geometric structure, as suggested previously [25].

2. Experimental and computational methods

2.1 Experimental setup

The experiments are performed in a cluster beam experiment connected to a beamline of the Infrared Free Electron Laser at the Fritz Haber Institute of the Max Planck Society in Berlin, Germany (FHI FEL) [45, 46]. The cluster experiment has been described before [47] and is upgraded here with a new dual-target dual-laser ablation source (Fig. 1), with a design similar to the one reported by Banser *et al.* [44].

Mixed boron-silicon clusters (Si_nB_m) are produced by laser ablation of a silicon rod (natural isotopic abundance, ESPI metals, US) and an isotopically-enriched ^{11}B rod (99.5%, Ceradyne, US; rod manufactured by RHP technology, Austria) within a pulsed flow of helium carrier gas. The two cylindrical rods with 6.2 mm diameter are symmetrically located on opposite sides of the central gas channel. This channel has a diameter of 6 mm, and its volume can be adjusted with a teflon tube insert. Each rod is translated and rotated by a separate mechanism containing an in-vacuum stepper motor and a worm gear with a transmission ratio of 34:1 between motor and rod. This leads to a smooth and very slow movement of the target (few hours for one turn if required), always providing a fresh target. For ablation, two pulsed Nd:YAG lasers (Continuum Minilite, 10 Hz, 532 nm, ~5 ns) are focused by lenses onto the targets. The two parallel laser beams from the backside of the source are deflected to hit each rod at an angle of 60° with respect to the channel axis. This design ensures good spatial overlap of the ablation plumes, which is crucial for stable and controllable formation of binary clusters [43]. A solenoid valve (General Valve Series 9) is used to provide short helium carrier gas pulses (several 100 µs) at a backing pressure of about 4 bar. Through three-body collisions with carrier gas atoms, the atomic and molecular species contained in the ablation plasma are cooled down and form clusters. By tuning the laser fluence on each rod, either bare cluster distributions or binary cluster distributions with arbitrary mixing ratio can be produced (Fig. 2). Typically, pulse energies of about 4-6 mJ are used for Si and 5-8 mJ for B. The source is extended with a thermally insulated thermalization and reaction channel of 3 mm inner diameter and 40 mm length. The inlet for reaction gases is not used in the experiments described here. The temperature of the channel can be stabilized between 80 and 400 K using a flow of liquid nitrogen and/or an electrical heater. In the experiments reported here it was set to 90 K. At the channel exit, a converging/diverging nozzle of ~1 mm aperture is mounted to induce further cooling [48].

The molecular beam is collimated by a skimmer with 2 mm diameter. Before passing through a 1 mm aperture located further downstream and held at ~200 V to deflect charged clusters, the neutral Si_nB_m clusters are irradiated with a counter-propagating IR laser beam from the FHI-FEL and then post-ionized after a delay of 30 µs by an unfocused F_2 excimer laser (photon energy E_{F2}=7.87 eV) in the extraction zone of a reflectron time-of-

flight mass spectrometer. The FHI FEL can deliver pulsed radiation in the wavelength range from 3.5 to 48 μm, with up to 100 mJ within a macropulse of ~7 μs duration at about 0.4-1% full width at half maximum (FWHM) bandwidth. In our experiments an electron beam energy of 26 MeV is used, providing access to a spectral range of 420-1100 cm^{-1}. If the frequency of the FEL radiation is resonant with an IR active mode of a specific cluster, it can absorb IR photons followed by rapid intracluster vibrational energy redistribution, and thereby its internal energy increases. The ionization efficiency usually follows a S-curve behavior as a function of excitation energy, with a slope depending on the Franck–Condon factor for ionization [49]. An increase in the internal energy of the cluster upon IR absorption therefore results in an enhancement of the ionization yield. An IR-UV2CI spectrum is obtained from the relative ionization enhancement normalized by the IR photon flux as a function of the IR laser frequency [25, 50, 51], which closely reflects the linear vibrational absorption spectrum of the neutral cluster.

2.2 Computational method

Quantum chemical calculations are performed to aid in the structural assignment and to give additional insight into electronic properties of the clusters. The most stable Si_6B structures are found with a genetic algorithm (GA) [52] coupled with DFT calculations, denoted as GA-DFT. Briefly, the GA-DFT approach starts with an initial population consisting of 32 candidate structures (individuals). Candidate structures are created by randomly distributing the atoms within a sphere with a radius of 1.9 Å ($r \approx r_0\, n^{1/3}$, n=7, r_0=1 Å). For each structure, the total energy obtained from local optimization at the RI-BP86/def-SVP level (TURBOMOLE V6.3.1 [53]) serves as the corresponding fitness value. After each generation, a new population is formed by tournament selection and subsequent modifications through crossover (p_{cross}=0.6) and mutation (p_{mut}=0.1) operators [54, 55]. Typically, up to a thousand candidate structures are evaluated. The first 20 non-equivalent low-energy isomers are then tightly optimized at the TPSS-D3/cc-pVTZ, B3LYP-D3/cc-pVTZ, and G4 levels (GAUSSIAN 09 [56]). At these levels, also IR spectra, vertical ionization energies (VIE), and natural bond orbital (NBO) populations are calculated. Relative energies are corrected for zero-point vibrational energies. No scaling factor is employed for vibrational frequencies [51]. The theoretical IR absorption stick spectra are convoluted with a Gaussian profile with FWHM=20 cm^{-1}. If not stated otherwise, the optimized parameters obtained at the TPSS level are given, while the B3LYP-D3 values are additionally given in parentheses.

3. Results and discussion

Parts of the mass distributions obtained by near-threshold photoionization of neutral clusters using the F_2 laser alone are shown in Fig. 2 for the mass range m/z 100-300. Almost arbitrary mixing ratios of Si_nB_m clusters can be achieved by just altering the laser pulse energies used for the ablation of the two targets. Pure Si_n clusters ($n \leq 20$, Fig. 2a) or pure B_m clusters ($m \leq 30$, Fig. 2d) are readily produced by ablation from just a single target, with observed distributions similar to what has been reported before [31, 57]. These distributions mainly reflect the variation in the ionization energies with cluster size. By increasing the laser pulse energy on the second target,

doping with single atoms or higher mixing ratios can be achieved in a controlled way. As examples, distributions of Si-rich Si_nB_m clusters containing typically up to m=3 boron atoms and B-rich Si_nB_m clusters containing up to n=2 silicon atoms are shown in Fig. 2b and 2c, respectively. Larger Si_nB_m clusters ($n+m \geq 20$) can also be generated. However, the isotope distribution of $^{28,29,30}Si$ complicates the assignment of the mass spectra. Note that a ^{11}B-enriched boron target is used here to simplify the isotope pattern. In addition to neutral clusters, the laser ablation source also produces charged, i.e. cationic and anionic, species.

Figure 3 illustrates the enhancement of certain ion signals when in addition to the UV pulse also IR radiation is applied. At an IR frequency of 531 cm^{-1}, about 70% enhancement of the Si_6B^+ ion intensity is observed for all isotopologues, indicating a resonant IR active vibrational mode of Si_6B at this frequency. By scanning the IR frequency and recording the ionization enhancement of Si_6B^+, an IR-UV2CI spectrum of the neutral cluster is obtained.

The IR-UV2CI spectrum recorded for Si_6B in the 420-1000 cm^{-1} range is compared in Fig. 4 to linear IR absorption spectra calculated for the five lowest-energy structures (**6a**-**6e**). These Si_6B isomers are found with the GA-DFT approach and are further optimized at the TPSS-D3/cc-pVTZ, B3LYP-D3/cc-pVTZ, and G4 levels. Their structural, vibrational, and energetic parameters are available in the Supporting Information (SI). Most of the computational results have already been provided in our recent work [25] and support the previous study of Tam *et al.* [19]. Generally, the three used methods agree in predicting the most stable structure (**6a**), while for the substantially higher-energy structures (≥30 kJ/mol) slight differences in their relative energies are observed. In addition to the molecular symmetries and electronic ground states (Fig. 4), the VIE values (TPSS level) are also shown to judge the possibility to detect the various isomeric clusters with the IR-UV2CI technique.

The most stable structure **6a** of Si_6B is a distorted pentagonal bipyramid (C_s, $^2A'$) formed by substituting a Si atom at an apex of the most stable Si_7 structure (D_{5h}, $^1A_1'$) by a B atom. Its VIE value of 8.0 eV is similar to E_{F2} (7.87 eV), indicating that **6a** can readily be detected if present in the molecular beam. According to the TPSS calculations, the next stable structure **6b** with C_{2v} ($^2A_1$) symmetry is 42 kJ/mol higher in energy and formed by B-substitution of a Si atom at the equator of the Si_7 pentagonal bipyramid. These most favorable locations for B-doping in Si_7 have previously been observed also for other dopant atoms, e.g., in Si_6C (C_{5v}) [25], Si_6V (C_{2v}), and Si_6Mn (C_{2v}) [58]. The other high-lying Si_6B structures **6c**-**6e** have a very similar topology, but differ in the location of the B atom. Except for **6a**, all structures have predicted VIE values (7.0-7.2 eV) well below E_{F2}, and thus would be, in case of their presence, more difficult to detect using the IR-UV2CI technique.

Within the investigated spectral range of 450-1000 cm^{-1}, the IR-UV2CI spectrum of Si_6B exhibits three distinct bands centered at 430 (**A**), 535 (**B**), and 661 (**C**) cm^{-1}, which can readily be assigned to vibrational transitions of the most stable structure **6a**. Its calculated linear IR spectrum agrees well with the observed IR-UV2CI spectrum with respect to both the position and relative IR intensity of the transitions. Specifically, the weak band **A** is assigned to the equatorial breathing mode (a') predicted at 421 cm^{-1}. Band **B** is attributed to the axial breathing mode (a') calculated at 540 cm^{-1}. Finally, the intense and somewhat broader band **C** is interpreted as the two overlapping axial bending fundamentals (a" and a') predicted at 649 and 663 cm^{-1}, respectively. Its larger width

(FWHM=52 cm^{-1}) compared to those of band **A** and **B** (~22 cm^{-1}) is consistent with its interpretation of two unresolved transitions split by 24 cm^{-1}. In general, the deviations of 9, 5, 12, and 2 cm^{-1} are well within the spectral resolution of the experimental approach. No spectral signatures of the less stable isomers **6b**-**6e** are detected in the measured IR-UV2CI spectrum, consistent with their high relative energy (and their low VIE values).

Interestingly, it is found that the five equivalent minima of Si_6B in the **6a** structure are separated by a very low barrier of only 0.7 kJ/mol at a C_s symmetric transition state (^{2}A", Figure S2), indicating fluxional behavior even at low temperature. However, it appears that the calculated harmonic spectrum reproduces the experimental one very well indicating an only minor role of anharmonic effects. Notably, the real part of the IR spectrum calculated for the transition state is nearly identical to the one of **6a**. Within the DFT calculations a C_{5v} symmetric $^2E_2$ state is found 16.9 kJ/mol higher in energy than **6a** but is expected to undergo symmetry-lowering due to the Jahn-Teller effect.

It is instructive to compare the properties of Si_6B with those of Si_7 [25, 27] to evaluate the effects of Si→B substitution on the geometric, vibrational, and electronic properties. To this end, Figure 5 shows the vibrational spectra and geometric structures of Si_7 and its B-doped counterpart Si_6B. At the first glance, the D_{5h} symmetry of the closed-shell Si_7 pentagonal bipyramid ($^1A_1$') is reduced to C_s symmetry for the open-shell Si_6B cluster (^{2}A'). Further, doping with a B atom makes Si_6B more compact in shape compared to Si_7, due to the stronger and shorter Si-B bonds as compared to the Si-Si bonds. Specifically, in the five-membered Si ring, the averaged Si-Si bond length is 2.367 (2.382) Å for Si_6B and 2.504 (2.515) Å for Si_7. In addition, the distance between the apex atoms is 2.270 (2.294) Å for Si_6B, much shorter than that for Si_7 (2.529 (2.570) Å). Boron doping has also a substantial impact on the appearance of the IR spectrum. In general, symmetry reduction produces a richer spectrum due to a larger number of IR allowed transitions, and the lighter mass of B and the larger force constants of the B-Si bonds result in higher vibrational frequencies. The bending mode of the axial atoms at 418 cm^{-1} (e_1') for Si_7 is split and shifted to 649 (a") and 663 cm^{-1} (a') for Si_6B. The IR-forbidden breathing mode of Si_7 at 437 cm^{-1} (a_1') becomes strongly IR-active for Si_6B and shifts to 540 cm^{-1} (a'). The NBO population analysis [59] shows that a large negative charge of -1.41 *e* (-1.45 *e*) is located on the electron-accepting B dopant atom, while the corresponding positive charge is nearly equally distributed over all Si atoms in the five-membered ring. Only an amount of 0.01 *e* (0.03 *e*) is located at the Si atom at the apex. In terms of electronic transitions, Si_6B shows the first allowed transition in the IR range (0.52 eV), whereas it is at 3.35 eV for Si_7 [25].

4. Conclusions

Binary boron-silicon clusters (Si_nB_m) are generated in a new dual-target dual-laser ablation source and characterized by means of mass spectrometry, IR-UV2CI spectroscopy, and quantum chemical simulations. By altering the laser fluences on the target rods, either Si-rich or B-rich clusters can be produced. With a predicted VIE value slightly higher than the F_2 laser photon energy, Si_6B is a suitable cluster for testing the capability of the new cluster source for coupling with IR-UV2CI spectroscopy. Three vibrational bands of Si_6B are observed

experimentally, in agreement with the calculated vibrational modes of the most stable isomer (**6a,** C_s, $^2A'$). Calculated VIE values of the five lowest-energy Si_6B isomers suggest that only **6a** may be detected by our IR-UV2CI setup under the present experimental conditions. However, as all these less stable isomers (**6b**-**6e**) are predicted to be rather high in energy, they are not expected to be produced in the cluster source. Comparing to Si_7, Si_6B is more compact in shape and exhibits optical absorption at much lower frequency (IR range). In general, our setup can be used to study binary clusters of metals, metalloids, and semiconductor elements, which is currently of great interest for searching novel cluster building blocks.

Acknowledgements

This work was supported by the Deutsche Forschungsgemeinschaft within the research unit FOR 1282 (DO 729/5, FI 893/4). We thank Philipp Jäger and Alex P. Woodham for their support in the experiments.

References

[1] M.J. Schoning, F. Ronkel, M. Crott, M. Thust, J.W. Schultze, P. Kordos, H. Luth, Miniaturization of potentiometric sensors using porous silicon microtechnology, Electrochim Acta, 42 (1997) 3185-3193.

[2] R.N. Barnett, U. Landman, Cluster-derived structures and conductance fluctuations in nanowires, Nature, 387 (1997) 788-791.

[3] K. Tomioka, M. Yoshimura, T. Fukui, A III-V nanowire channel on silicon for high-performance vertical transistors, Nature, 488 (2012) 189-192.

[4] T.M. Fu, X.J. Duan, Z. Jiang, X.C. Dai, P. Xie, Z.G. Cheng, C.M. Lieber, Sub-10-nm intracellular bioelectronic probes from nanowire-nanotube heterostructures, Proc. Natl. Acad. Sci. U.S.A., 111 (2014) 1259-1264.

[5] N.M. Ravindra, The drive for further miniaturization: Silicon nanoelectronics, Jom-Us, 57 (2005) 14-15.

[6] W. de Heer, The physics of simple metal clusters: experimental aspects and simple models, Rev. Mod. Phys., 65 (1993) 611-676.

[7] T.P. Martin, NATO, Large clusters of atoms and molecules, Kluwer, Dordrecht, 1996.

[8] P. Melinon, B. Masenelli, F. Tournus, A. Perez, Playing with carbon and silicon at the nanoscale, Nat Mater, 6 (2007) 479-490.

[9] C. Ray, M. Pellarin, J.L. Lerme, J.L. Vialle, M. Broyer, X. Blase, P. Melinon, P. Keghelian, A. Perez, Synthesis and structure of silicon-doped heterofullerenes, Phys. Rev. Lett., 80 (1998) 5365-5368.

[10] J. Nagamatsu, N. Nakagawa, T. Muranaka, Y. Zenitani, J. Akimitsu, Superconductivity at 39 K in magnesium diboride, Nature, 410 (2001) 63-64.

[11] E.A. Ekimov, V.A. Sidorov, E.D. Bauer, N.N. Mel'nik, N.J. Curro, J.D. Thompson, S.M. Stishov, Superconductivity in diamond, Nature, 428 (2004) 542-545.

[12] T. Yokoya, T. Nakamura, T. Matsushita, T. Muro, Y. Takano, M. Nagao, T. Takenouchi, H. Kawarada, T. Oguchi, Origin of the metallic properties of heavily boron-doped superconducting diamond, Nature, 438 (2005) 647-650.

[13] E. Bustarret, C. Marcenat, P. Achatz, J. Kacmarcik, F. Levy, A. Huxley, L. Ortega, E. Bourgeois, X. Blase, D. Debarre, J. Boulmer, Superconductivity in doped cubic silicon, Nature, 444 (2006) 465-468.

[14] T. Muranaka, Y. Kikuchi, T. Yoshizawa, N. Shirakawa, J. Akimitsu, Superconductivity in carrier-doped silicon carbide, Sci. Technol. Adv. Mat., 9 (2008) 044204.

[15] M. Kriener, Y. Maeno, T. Oguchi, Z.A. Ren, J. Kato, T. Muranaka, J. Akimitsu, Specific heat and electronic states of superconducting boron-doped silicon carbide, Phys. Rev. B., 78 (2008) 024517.

[16] Z.A. Ren, J. Kato, T. Muranaka, J. Akimitsu, M. Kriener, Y. Maeno, Superconductivity in boron-doped SiC, J. Phys. Soc. Jpn, 76 (2007) 103710.

[17] K. Iakoubovskii, Superconductivity in covalent semiconductors, Cent. Eur. J. Phys., 7 (2009) 654-662.

[18] P.H. Dai, Y.H. Zhang, M.P. Sarachik, Critical Conductivity Exponent for Si-B, Phys. Rev. Lett., 66 (1991) 1914-1917.

[19] N.M. Tam, T.B. Tai, M.T. Nguyen, Thermochemical Parameters and Growth Mechanism of the Boron-Doped Silicon Clusters, Si_nB^q with n=1-10 and q =-1, 0,+1, J. Phys. Chem. C, 116 (2012) 20086-20098.

[20] N.T. Bagraev, W. Gehlhoff, L.E. Klyachkin, A.M. Malyarenko, V.V. Romanov, S.A. Rykov, Superconductivity in silicon nanostructures, Physica C, 437-38 (2006) 21-24.

[21] A. Grockowiak, T. Klein, H. Cercellier, F. Levy-Bertrand, X. Blase, J. Kacmarcik, T. Kociniewski, F. Chiodi, D. Debarre, G. Prudon, C. Dubois, C. Marcenat, Thickness dependence of the superconducting critical temperature in heavily doped Si:B epilayers, Phys. Rev. B., 88 (2013) 064508.

[22] R. Viswanathan, R.W. Schmude, K.A. Gingerich, Thermochemistry of BSi(g), BSi_2(g), and BSi_3(g), J. Phys. Chem., 100 (1996) 10784-10786.

[23] R. Davy, E. Skoumbourdis, D. Dinsmore, Structure, energies, vibrational spectra and reactions of the boron-silicon cluster molecules B_2Si, BSi_2 and B_2Si_2, Mol. Phys., 103 (2005) 611-619.

[24] Z. Sun, Z. Yang, Z. Gao, Z.C. Tang, Experimental and theoretical investigation on binary semiconductor clusters of B/Si and Al/Si, Rapid Commun. Mass. Sp., 21 (2007) 792-798.

[25] N.X. Truong, M. Savoca, D.J. Harding, A. Fielicke, O. Dopfer, Vibrational spectra and structures of neutral Si_6X clusters (X = Be, B, C, N, O), Phys. Chem. Chem. Phys., 16 (2014) 22364-22372.

[26] T.B. Tai, P. Kadlubanski, S. Roszak, D. Majumdar, J. Leszczynski, M.T. Nguyen, Electronic Structures and Thermochemical Properties of the Small Silicon-Doped Boron Clusters B_nSi (n=1-7) and Their Anions, Chem. Phys. Chem., 12 (2011) 2948-2958.

[27] A. Fielicke, J.T. Lyon, M. Haertelt, G. Meijer, P. Claes, J. de Haeck, P. Lievens, Vibrational spectroscopy of neutral silicon clusters via far-IR-VUV two color ionization, J Chem Phys, 131 (2009) 171105.

[28] Y.J. Li, N.M. Tam, P. Claes, A.P. Woodham, J.T. Lyon, V.T. Ngan, M.T. Nguyen, P. Lievens, A. Fielicke, E. Janssens, Structure Assignment, Electronic Properties, and Magnetism Quenching of Endohedrally Doped Neutral Silicon Clusters, Si_nCo (n=10-12), J. Phys. Chem. A, 118 (2014) 8198-8203.

[29] M. Haertelt, J.T. Lyon, P. Claes, J. de Haeck, P. Lievens, A. Fielicke, Gas-phase structures of neutral silicon clusters, J Chem Phys, 136 (2012) 064301.

[30] M. Savoca, A. Lagutschenkov, J. Langer, D.J. Harding, A. Fielicke, O. Dopfer, Vibrational Spectra and Structures of Neutral Si_mC_n Clusters (m + n=6): Sequential Doping of Silicon Clusters with Carbon Atoms, J. Phys. Chem. A, 117 (2013) 1158-1163.

[31] C. Romanescu, D.J. Harding, A. Fielicke, L.S. Wang, Probing the structures of neutral boron clusters using infrared/vacuum ultraviolet two color ionization: B_{11}, B_{16}, and B_{17}, J Chem Phys, 137 (2012) 014317.

[32] C. Romanescu, T.R. Galeev, A.P. Sergeeva, W.L. Li, L.S. Wang, A.I. Boldyrev, Experimental and computational evidence of octa- and nona-coordinated planar iron-doped boron clusters: $Fe(c)B_8^-$ and $Fe(c)B_9^-$, J. Organomet. Chem., 721 (2012) 148-154.

[33] M.A. Duncan, Invited review article: laser vaporization cluster sources, Rev. Sci. Instrum., 83 (2012) 041101.

[34] R.G. Wheeler, K. Laihing, W.L. Wilson, J.D. Allen, R.B. King, M.A. Duncan, Neutral Gas-Phase Analogs of Condensed-Phase Post-Transition-Metal Cluster Ions - Laser Vaporization and Photoionization of Sn/Bi and Pb/Sb Alloys, J. Am. Chem. Soc., 108 (1986) 8101-8102.

[35] T. Kimura, T. Sugai, H. Shinohara, Production and characterization of boron- and silicon-doped carbon clusters, Chem. Phys. Lett., 256 (1996) 269-273.

[36] A. Nakajima, T. Taguwa, K. Nakao, M. Gomei, R. Kishi, S. Iwata, K. Kaya, Photoelectron spectroscopy of silicon-carbon cluster anions, Surf. Rev. Lett., 3 (1996) 411-415.

[37] M. Pellarin, C. Ray, P. Melinon, J. Lerme, J.L. Vialle, P. Keghelian, A. Perez, M. Broyer, Silicon-carbon mixed clusters, Chem. Phys. Lett., 277 (1997) 96-104.

[38] H.T. Deng, B.C. Guo, K.P. Kerns, A.W. Castleman, Formation and Stability of Metallocarbohedrenes - $Ti_xM_yC_{12}$ (x+y=8, M=Nb, Ta, Y, and Si), Int. J. Mass. Spectrom., 138 (1994) 275-281.

[39] C. Romanescu, T.R. Galeev, W.L. Li, A.I. Boldyrev, L.S. Wang, Aromatic Metal-Centered Monocyclic Boron Rings: $Co(c)B_8^-$ and $Ru(c)B_9^-$, Angew. Chem. Int. Edit., 50 (2011) 9334-9337.

[40] S. Nonose, Y. Sone, K. Onodera, S. Sudo, K. Kaya, Structure and Reactivity of Bimetallic Co_nV_m Clusters, J. Phys. Chem., 94 (1990) 2744-2746.

[41] R.L. Wagner, W.D. Vann, A.W. Castleman, A technique for efficiently generating bimetallic clusters, Rev. Sci. Instrum., 68 (1997) 3010-3013.

[42] W. Bouwen, P. Thoen, F. Vanhoutte, S. Bouckaert, F. Despa, H. Weidele, R.E. Silverans, P. Lievens, Production of bimetallic clusters by a dual-target dual-laser vaporization source, Rev. Sci. Instrum., 71 (2000) 54-58.

[43] K. Koyasu, J. Atobe, M. Akutsu, M. Mitsui, A. Nakajima, Electronic and geometric stabilities of clusters with transition metal encapsulated by silicon, J. Phys. Chem. A, 111 (2007) 42-49.

[44] D. Banser, M. Schnell, J.U. Grabow, E.J. Cocinero, A. Lesarri, J.L. Alonso, The internuclear potential, electronic structure, and chemical bond of tellurium selenide, Angew. Chem. Int. Edit., 44 (2005) 6311-6315.

[45] W. Schöllkopf, S. Gewinner, H. Junkes, A. Paarmann, G. von Helden, H. Bluem, A.M.M. Todd, The new IR and THz FEL Facility at the Fritz Haber Institute in Berlin, in: SPIE Conference *Advances in X-ray Free-Electron Lasers Instrumentation III*, Sandra G. Biedron, Editor, Proc. of SPIE 9512, 2015, 95121L.

[46] W. Schöllkopf, S. Gewinner, W. Erlebach, H. Junkes, A. Liedke, G. Meijer, A. Paarmann, G. von Helden, H. Bluem, D. Dowell, R. Lange, J. Rathke, A.M.M. Todd, L.M. Young, U. Lehnert, P. Michel, W. Seidel, R. Wünsch, S.C. Gottschalk, The new IR FEL Facility at the Fritz-Haber-Institut in Berlin, in: Proc. of the 36th Free Electron Laser Conference, Basel, Switzerland, 2014, pp. 629 – 634.

[47] A. Fielicke, G. von Helden, G. Meijer, Far-infrared spectroscopy of isolated transition metal clusters, Eur. Phys. J. D, 34 (2005) 83-88.

[48] H. Pauly, Atom, molecule, and cluster beams I basic theory, production and detection of thermal energy beams, Springer, Berlin, 2000.

[49] A.S. Sudbo, P.A. Schulz, D.J. Krajnovich, Y.T. Lee, Y.R. Shen, Photo-Ionization Study of Multiphoton-Excited SF_6 in a Molecular-Beam, Opt. Lett., 4 (1979) 219-221.

[50] M. Haertelt, A. Fielicke, G. Meijer, K. Kwapien, M. Sierka, J. Sauer, Structure determination of neutral MgO clusters-hexagonal nanotubes and cages, Phys. Chem. Chem. Phys., 14 (2012) 2849-2856.

[51] N.X. Truong, M. Savoca, D.J. Harding, A. Fielicke, O. Dopfer, Vibrational spectra and structures of Si_nC clusters (n = 3-8), Phys. Chem. Chem. Phys., 17 (2015) 18961-18970.

[52] M. Wall, GAlib: A C++ Genetic Algorithm Library. Available from: http://lancet.mit.edu/ga.

[53] TURBOMOLE V6.3 2011, a development of University of Karlsruhe and Forschungszentrum Karlsruhe GmbH, 1989-2007, TURBOMOLE GmbH, since 2007. Available from http://www.turbomole.com.

[54] D.E. Goldberg, Genetic algorithms in search, optimization, and machine learning, Addison-Wesley, Reading, Mass. ; Wokingham, 1989.

[55] J.H. Holland, Adaptation in natural and artificial systems : an introductory analysis with applications to biology, control, and artificial intelligence, 1st MIT Press ed., MIT Press, 1992.

[56] M.J. Frisch, G.W. Trucks, H.B. Schlegel, G.E. Scuseria, M.A. Robb, J.R. Cheeseman, G. Scalmani, V. Barone, B. Mennucci, G.A. Petersson, H. Nakatsuji, M. Caricato, X. Li, H.P. Hratchian, A.F. Izmaylov, J. Bloino, G. Zheng, J.L. Sonnenberg, M. Hada, M. Ehara, K. Toyota, R. Fukuda, J. Hasegawa, M. Ishida, T. Nakajima, Y. Honda, O. Kitao, H. Nakai, T. Vreven, J.A. Montgomery, Jr., J.E. Peralta, F. Ogliaro, M. Bearpark, J.J. Heyd, E. Brothers, K.N. Kudin, V.N. Staroverov, R. Kobayashi, J. Normand, K. Raghavachari, A. Rendell, J.C. Burant, S.S. Iyengar, J. Tomasi, M. Cossi, N. Rega, N.J. Millam, M. Klene, J.E. Knox, J.B. Cross, V. Bakken, C. Adamo, J. Jaramillo, R. Gomperts, R.E. Stratmann, O. Yazyev, A.J. Austin, R. Cammi, C. Pomelli, J.W. Ochterski, R.L. Martin, K. Morokuma, V.G. Zakrzewski, G.A. Voth, P. Salvador, J.J. Dannenberg, S. Dapprich, A.D. Daniels, Ö. Farkas, J.B. Foresman, J.V. Ortiz, J. Cioslowski, D.J. Fox, Gaussian 09 Revision D.01, in, Gaussian Inc. Wallingford CT, 2009.

[57] D.J. Trevor, D.M. Cox, K.C. Reichmann, R.O. Brickman, A. Kaldor, Ionizing Laser Intensity Dependence of the Silicon Cluster Photoionization Mass-Spectrum, J. Phys. Chem., 91 (1987) 2598-2601.

[58] P. Claes, V.T. Ngan, M. Haertelt, J.T. Lyon, A. Fielicke, M.T. Nguyen, P. Lievens, E. Janssens, The structures of neutral transition metal doped silicon clusters, Si_nX (n=6-9; X = V, Mn), J Chem Phys, 138 (2013) 194301.

[59] F.L. Weinhold, Clark R., Discovering Chemistry With Natural Bond Orbitals, John Wiley & Sons, Inc., Canada, 2012.

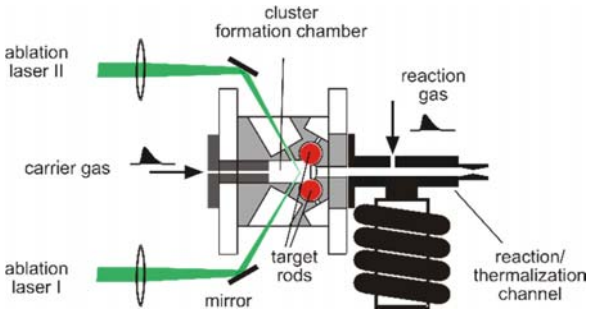

Figure 1. Schematic view of the dual-target dual-laser ablation source for the production of mixed Si_nB_m clusters.

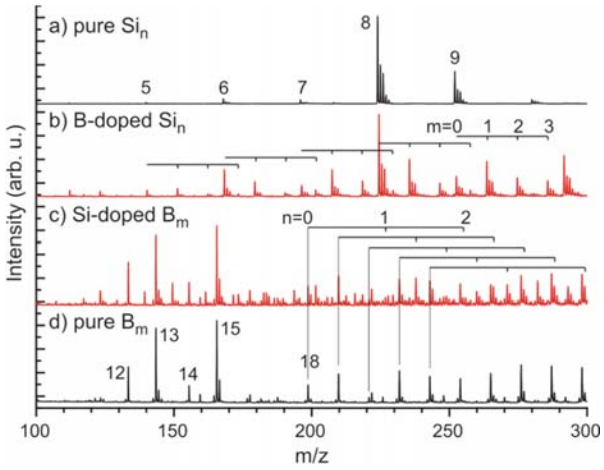

Figure 2. Typical mass spectra of Si_nB_m mixed clusters produced with the dual-target dual-laser ablation source. By altering the laser fluences, arbitrary mixing ratios of Si_nB_m clusters, i.e., from pure Si_n and B_m to Si-rich and B-rich Si_nB_m can be achieved. The used laser pulse energies are $^{Si}E_{abl}/^{B}E_{abl}$ = 6/0 mJ (a), 6/6 mJ (b), 6/8 mJ (c), and 0/8 mJ (d).

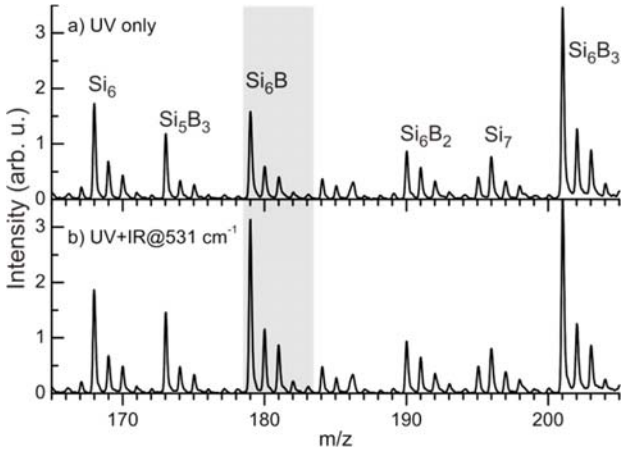

Figure 3. Mass spectra of Si_nB_m clusters irradiated with a) UV laser only and b) UV and IR radiation at a frequency of 531 cm^{-1}, showing a significant enhancement (~70%) of the Si_6B ion yield with the additional IR radiation.

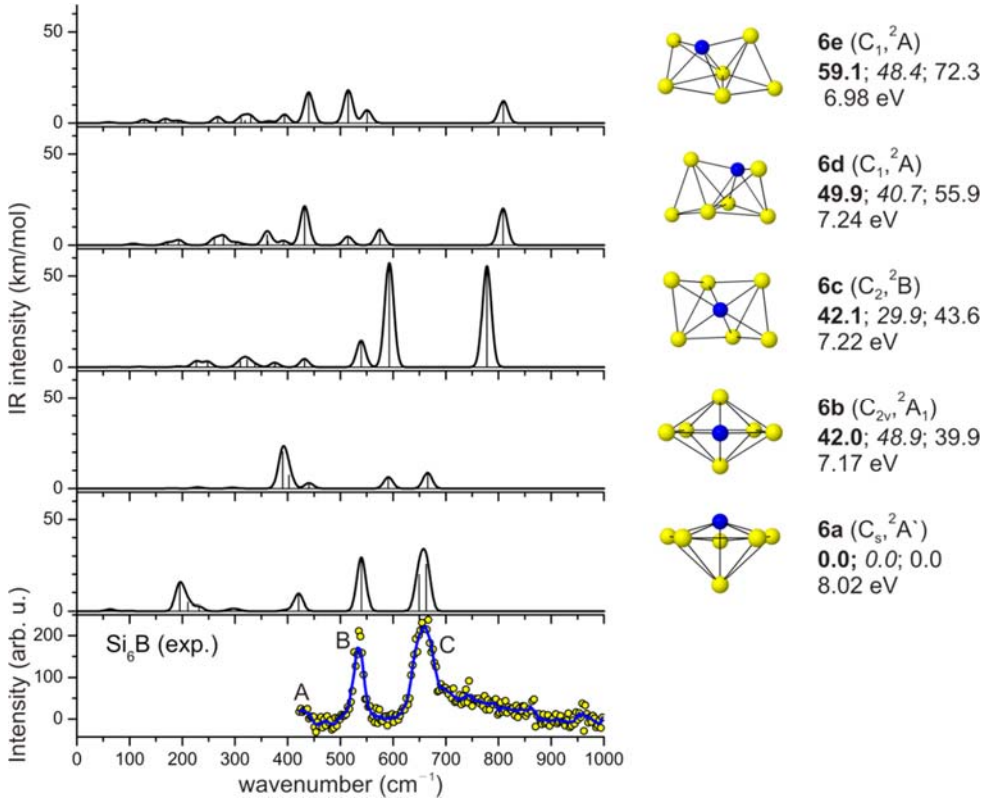

Figure 4. Comparison of the IR-UV2CI spectrum recorded for Si_6B with the vibrational spectra of the five lowest-energy structures **6a-6e** calculated at the TPSS-D3/cc-pVTZ level. Experimental peak positions are 430 (**A**, onset), 535 (**B**), and 661 (**C**) cm^{-1}. The relative energies obtained at the TPSS-D3/cc-pVTZ, B3LYP-D3/cc-pVTZ, and G4 levels are given in kJ/mol (left to right), along with point group symmetries, electronic states, and vertical ionization energies (VIE in eV) obtained at the TPSS-D3 level. Cartesian coordinates and vibrational spectra of the calculated structures are provided in the Supporting Information.

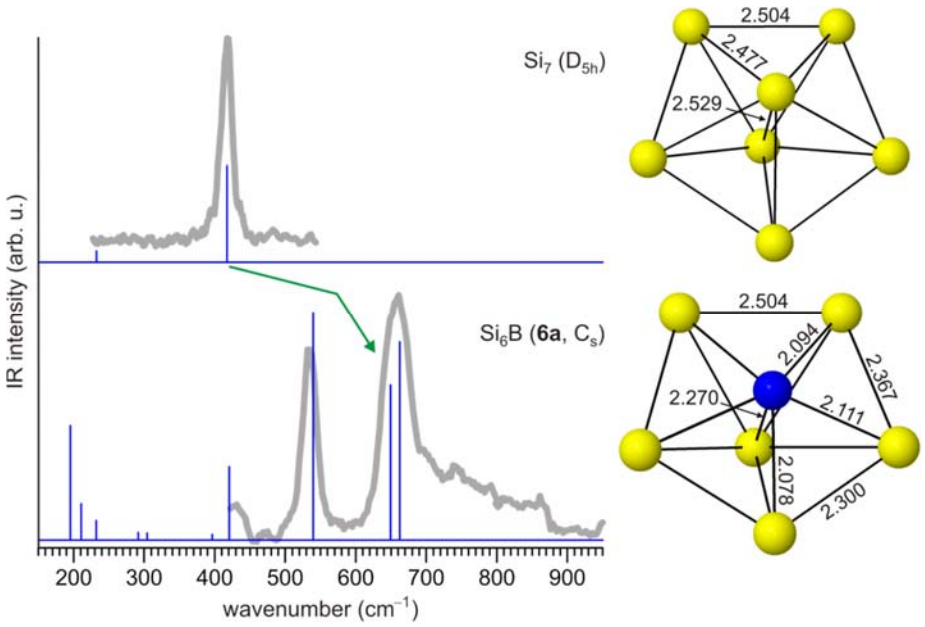

Figure 5. Ground state structures and IR spectra of Si_7 (D_{5h}) and Si_6B (C_s) clusters calculated at the TPSS-D3 level compared to the IR-UV2CI spectra. The green arrow marks the shift and splitting of the degenerate axial bending mode when a Si atom is substituted by a B atom in the Si_7 cluster. Bond lengths are given in Å.